

## Space-Charge-Limited Currents in Iodine Single Crystals

A. MANY,\* S. Z. WEISZ, AND M. SIMHONY  
*Department of Physics, The Hebrew University, Jerusalem, Israel*

(Received January 17, 1962)

Transient and steady-state measurements of space-charge-limited hole photocurrents in iodine generated at one electrode are presented. The hole drift mobility perpendicular to the *ac* crystallographic plane is  $0.7 \text{ cm}^2/\text{v sec}$  and varies with temperature approximately at  $T^{-1.2}$ . The transient measurements are compared with the theory presented in the preceding paper and found to be in very good agreement with it in regard to both transport phenomena and trapping processes. This theory is employed in the analysis of the experimental data to characterize the hole trapping kinetics. Trapping times derived in this manner range from tens of microseconds to seconds, depending on the crystal-growth conditions and subsequent treatment. These conditions affect also the location of the dominant trapping levels above the valence-band edge and their density, which, for different samples, range from 0.45 to 0.6 eV and from  $10^{11}$  to  $10^{14} \text{ cm}^{-3}$ , respectively. The hole capture cross sections are usually very small, of the order of  $10^{-20} \text{ cm}^2$ .

### I. INTRODUCTION

IN a previous paper<sup>1</sup> studies of photoconductivity in iodine have been reported, together with some preliminary results of space-charge-limited photocurrents (SCLC) in this material. A simplified theory of transient SCLC in insulators which omits trapping effects, has been developed and found to account well for those features of the experimental data which were not appreciably affected by trapping. The present paper compliments these preliminary results, with particular emphasis on trapping effects. The detailed theory of transient SCLC presented in the preceding paper<sup>2</sup> is employed in the analysis of the experimental data. Such an analysis, especially when combined with that of steady-state SCLC measurements, enables a rather detailed characterization of transport and trapping processes in iodine.

Iodine forms molecular crystals which belong to the base-centered orthorhombic system. It has a low melting point ( $114^\circ\text{C}$ ) and a high vapor pressure at room temperature (0.2 mm Hg). Iodine is essentially an insulator, with resistivity of  $10^{11} \text{ ohm-cm}$  at room temperature. The resistivity varies exponentially with temperature with an activation energy of about 1 eV. Thermoelectric-power measurements suggest that the crystals studied are *p* type.

The spectral photoresponse of iodine consists of two sensitivity bands, a main band extending between  $0.35 \mu$  and  $0.55 \mu$  and a much weaker one centered at  $0.8 \mu$ . Photoconductive processes are of interest in the present paper only to the extent that light is able to generate the large carrier reservoir near one electrode, necessary to produce "ohmic"-contact conditions. Once these conditions are established, the photocurrent perpendicular to the illuminated surface is governed by space-charge limitation only, and is essentially independent of the detailed photoconductive processes.

Most of the results presented here are for these latter conditions. All current measurements are in a direction perpendicular to the *ac* crystallographic plane.

The phenomenological behavior of iodine as far as transport, recombination, and trapping processes are concerned, is found to be similar to that of covalent or ionic crystals; the difference lies mainly in the order of magnitude of the characteristic parameters involved. For the sake of convenience, the results presented would accordingly be discussed in terms of the band model, even though the band approximation is probably a poor one for such a molecular solid.

### II. EXPERIMENTAL TECHNIQUE

The samples studied are sublimated crystal-wafers obtained from commercially pure iodine (A.C.S. specifications). Due to the large vapor pressure of the material, the samples are hermetically sealed between two glass plates in a sandwich-type configuration. One plate has a coating of transparent tin oxide and serves as the ohmic (injecting) contact under illumination. The opposite side of the wafer is provided with a platinum electrode, surrounded by a guard ring to eliminate the large surface-leakage currents common in iodine. The absence of both rectification and photovoltage, and the characteristics of the current response to pulses, indicate that these contacts are effectively neutral, i.e., the energy bands at the interface remain flat at least to within a tunneling distance.

In the transient measurements, voltage pulses of variable amplitude (0-1000 v) and duration (0.1-30 msec) are applied to the sandwich cell, in series with a 15-kohm cathode-follower grid resistor. Two modes of illumination are employed. In the first, a short intense flash-light (duration  $\sim 0.2 \mu\text{sec}$ ) obtained from a xenon discharge tube is focused on the sample. The discharge is triggered by each voltage pulse following a variable time delay. For this mode of illumination, dc voltages can, in principle, be equally well employed. Pulse techniques are, however, more convenient in many respects. They are particularly useful when a blocking electrode is used, and, in general, for materials in which

\* Present address: RCA Laboratories, Princeton, New Jersey.

<sup>1</sup> A. Many, M. Simhony, S. Z. Weisz, and J. Levinson, International Conference on Photoconductivity, Cornell University, August, 1961 [J. Phys. Chem. Solids **22**, 285 (1961)].

<sup>2</sup> A. Many and G. Rakavy, preceding paper [Phys. Rev. **126**, 1980 (1962)].

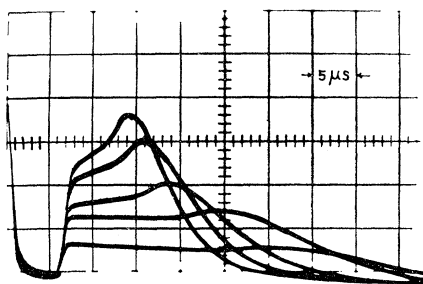


Fig. 1. Oscillograms of transient SCLC under intense *flash* illumination, for various applied voltages. The time scale ( $5 \mu\text{sec}/\text{cm}$ ) is common to all traces. The amplifier gain has been changed to get all traces on the same picture.

neutral contacts are not feasible. In the other mode of illumination, intense *steady* light from a Mazda high-pressure mercury lamp is employed. Here, the large carrier-reservoir characteristic of an ohmic contact is continually generated by the steady light. The applied voltage pulse injects carriers from this reservoir into the bulk, to constitute the transient SCLC. This configuration is analogous to that of an ohmic metal-insulator contact, such as indium on cadmium sulfide<sup>3</sup>.

The transient photocurrent is amplified and displayed on a Tektronix CRO. The over-all circuitry response time is  $\sim 1 \mu\text{sec}$  for the case of flash illumination. For steady illumination, it is somewhat longer due to the large capacitive disturbance at the onset of the voltage pulse.

For steady-state measurements, the same mercury light source is employed. The photosignal is fed via a breaker amplifier to a recorder. In this manner, the slow decay component of the photocurrent following the application of the dc voltage may be studied, and the asymptotic steady value determined.

In all cases the spectral composition of the light corresponds to the main photosensitivity band of iodine, for which the absorption coefficient is  $10^4 \text{ cm}^{-1}$  or larger. This ensures that the carriers are generated very close to the illuminated electrode.

### III. GENERAL CHARACTERISTICS OF THE TRANSIENT SCLC

Typical oscillograms of transient space-charge-limited photocurrents in iodine are shown in Figs. 1 and 2 for various applied voltages. The traces correspond to the illuminated electrode positive. For the reverse polarity, the photosignal is smaller by a factor of at least  $10^3$ , indicating that hole conduction largely predominates over electron conduction. The traces in each picture are on a common time base but with different amplifier gains. Fig. 1 represents the photocurrent resulting from an intense *flash* illumination of the transparent electrode while Figs. 2(a) and (b) represent (on two time scales) the photocurrent arising from the voltage pulse in the presence of intense steady illumi-

nation. The general characteristics of the photocurrent are just those predicted by theoretical considerations.<sup>1,2</sup> Due to space-charge effects, only a relatively small portion of the reservoir generated by the intense light is allowed to be injected at any time into the bulk. Initially, the SCLC rises to an amplitude which, provided the reservoir is large enough, is independent of light intensity. As more and more carriers are being injected, the current gradually rises above this value, until the first front of carriers reaches the opposite electrode. Following this transit time, the current decays gradually to its steady-state value. In practice this behavior would be modified due to the accumulation of charge in traps. In the case of *flash* illumination an additional, much more important factor enters, namely, the dwindling with time of the carrier reservoir due to sweep-out effects and hole-electron recombination at the illuminated surface. Inspection of Fig. 1(a) shows that the photocurrent decays much faster for this mode of illumination. It is thus evident that for the study of bulk trapping processes, steady illumination must be employed in order to continually reinforce the carrier reservoir necessary to maintain an ohmic contact. Due, however, to the relatively large initial disturbance caused by the capacitive surge in the latter case, the measurement of the *initial* amplitude of the SCLC, as well as the carrier transit-time, is more accurately carried out by the flash-illumination technique. These quantities are almost unaffected by either bulk trapping or the dwindling of the carrier reservoir.

It is of interest to obtain an estimate of the magnitude of the photogenerated carrier reservoir for the two modes of illumination employed. Measurements of the

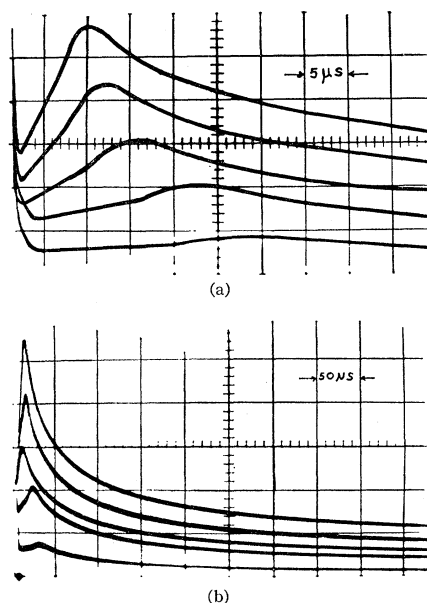


Fig. 2. Oscillograms of transient SCLC under intense *steady* illumination for the same applied voltages and amplifier gains as in Fig. 1. The time scale is  $5 \mu\text{sec}/\text{cm}$  for (a) and  $50 \mu\text{sec}/\text{cm}$  for (b).

<sup>3</sup> R. W. Smith and A. Rose, Phys. Rev. **97**, 1531 (1955).

photocurrent may be used toward this end only for the case of very weak light intensities, when space-charge effects are negligible. Using flash illumination of known photon flux, one obtains for the quantum efficiency  $\sim 0.02$ , from which the magnitude of the reservoir generated at any light intensity may be calculated. Measurement of the transient photocurrent under weak *steady* illumination, on the other hand, yields the steady-state carrier lifetime at the surface. The values obtained for this lifetime are of the order of  $50 \mu\text{sec}$ . The carrier reservoir under intense illumination estimated by use of these techniques is  $10^{10}$ – $10^{11} \text{ cm}^{-2}$ .

#### IV. TRANSPORT PHENOMENA

According to the mathematical analysis,<sup>1,2</sup> the *initial* amplitude of the transient SCLC density is given by

$$j(0) = 4.4 \times 10^{-14} \kappa \mu V^2 / L^3 \text{ amp/cm}^2, \quad (1)$$

where  $\kappa$  is the relative dielectric constant,  $\mu$  the hole mobility,  $L$  the sample thickness, and  $V$  the applied voltage. The transit time of the first front of carriers is given by

$$t_1 = 2(1 - e^{-\frac{1}{2}})(L^2 / \mu V) \approx 0.8 t_0, \quad (2)$$

$t_0 \equiv L^2 / \mu V$  being the transit time for space-charge *free* flow.

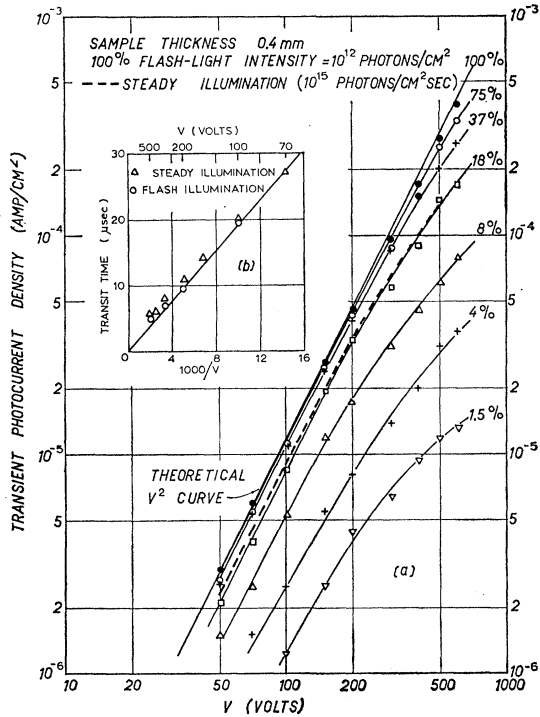


FIG. 3. (a) Initial amplitude of the transient photocurrent density plotted against applied voltage. Solid curves correspond to various light flash intensities, dashed curve to steady intense illumination. The upper curve is calculated from Eq. (1) using  $\mu = 0.7 \text{ cm}^2/\text{v sec}$  and  $\kappa = 2$ . (b) Transit time vs  $1000/V$  for steady (triangles) and flash (circles) illumination. Calculated mobility  $0.7 \text{ cm}^2/\text{v sec}$ .

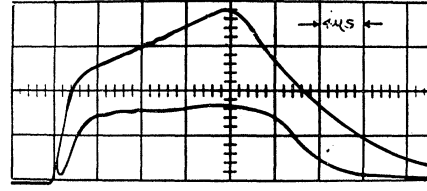


FIG. 4. Oscillograms of transient photocurrent for strong (upper curve) and weak flash-light intensities, demonstrating flow in the presence of and in the absence of space-charge effects. (The amplifier gain for the latter case is about 20 times larger).

Figure 3(a) represents log-log plots of the *initial* amplitude of the photocurrent density vs applied voltage for various light-flash intensities. For strong light and low applied voltages the initial current varies as  $V^2$  and is insensitive to light intensity, in agreement with Eq. (1). The agreement is similarly good for the case of *steady* illumination, as shown by the dashed curve. In Fig. 3(b) the measured transit time is plotted as a function of  $1000/V$  for both flash and steady illumination. The hole drift mobility, as determined by use of Eq. (2) is  $0.7 \text{ cm}^2/\text{v sec}$ . For diminishing light intensity and higher voltages, the reservoir at the illuminated anode can no longer supply the full value prescribed by Eq. (1), and the photocurrent approaches the value corresponding to space-charge free flow. The transit time should then approach  $t_0$ . This is demonstrated by the two oscillograms in Fig. 4 which correspond to space-charge-limited (intense light) and space-charge-free (weak light) flow. The transit time in the latter case

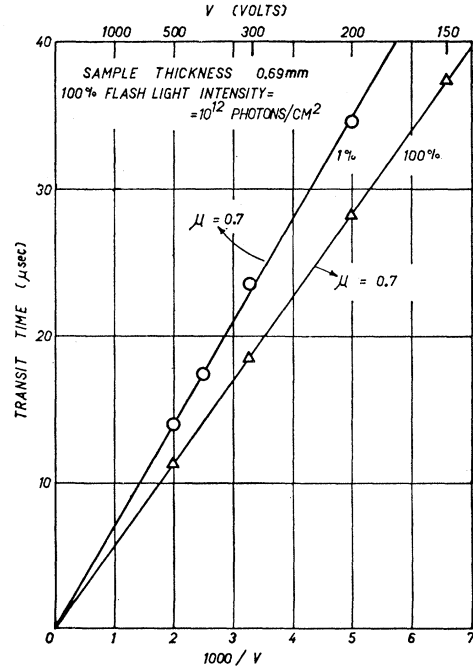


FIG. 5. Transit time vs  $1000/V$  for strong (triangle) and weak (circles) incident flash-light intensities. The ratio of the slopes of the lines is approximately 0.8.

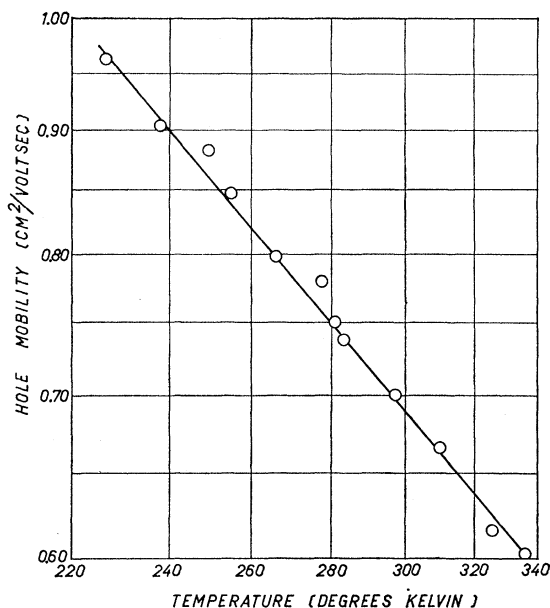


FIG. 6. Temperature dependence of the hole mobility, on a log-log scale. The slope is  $-1.2$ .

is seen to be about 20% longer than for the former. The measured transit-times for the two cases are plotted in Fig. 5 as a function of  $1000/V$ , the ratio of the slopes being very nearly 0.8, as required by Eq. (2).

The temperature dependence of the drift mobility is shown in Fig. 6 on a log-log scale. In contrast to what has been reported previously,<sup>1</sup> these more careful measurements show that the hole mobility varies approximately as  $T^{-1.2}$ . A similar temperature dependence has been reported for anthracene<sup>4</sup>.

A demonstration of the space-charge-limited nature of the transient photocurrent is given in Fig. 7. Here the initial amplitude of the transient SCLC density (corresponding to intense flash illumination) for different samples, measured at 100 v, is plotted (circles) against the third power of their thickness  $L$ , on a log-log scale. The solid curve is a plot of Eq. (1) using the independently determined values of the mobility and dielectric constant<sup>1</sup> ( $\kappa=2$ ). It is seen that the agreement between the experimental points and the theoretical curve is very good, as regards both slope ( $-1$ ) and absolute magnitude.

#### IV. TRAPPING PROCESSES

##### (a) Transient Measurements

Measurements of the transient SCLC arising from an applied voltage pulse, when the anode is illuminated by intense steady light, as illustrated by the oscillograms of Fig. 2, have been carried out on a large number of iodine samples. The samples differed widely both as regards their mode of preparation and subsequent treatment.

<sup>4</sup> R. G. Kepler, Phys. Rev. **119**, 1226 (1960).

A remarkable characteristic common to most samples was the surprisingly weak trapping effects exhibited by them. In a future publication, a study of the effect of crystal imperfections on trapping processes will be discussed. In the present paper we only present two extreme cases, one corresponding to a sample characterized by very weak trapping, the other by relatively prominent trapping. These two cases are shown in Figs. 8 and 9, respectively. The results in Figs. 8(a) and 9 are presented in dimensionless form, with the time axis expressed in units of the transit time  $t_1$ , and the current-density axis in terms of the initial value  $j(0)$ . In Fig. 8(a) the points represent measurements at three applied voltages, while the solid curve is the theoretical SCLC for the case of no trapping, i.e., for an infinite trapping time  $\tau$ , as calculated from Eqs. (27) and (37) of the preceding paper.<sup>2</sup> It is seen that the agreement is quite good, indicating that for the time scale of Fig. 8(a) ( $t_1$  being equal to 32, 16, and 8  $\mu$ sec for an applied voltage of 200, 400, and 800 v, respectively), trapping effects are still negligible ( $\tau \gg t_1$ ). The subsequent, much slower decay of the SCLC density for the three applied voltages is represented in Fig. 8(b) on a semi-log scale by the corresponding points. The decay is composed of two components (the dashed lines), one with a time constant of 0.55 sec, the other with a much longer time constant, in the minutes range, extending up to the steady-state value [about two percent of  $j(0)$ ]. The solid curve for each voltage is the sum of the corresponding two components and is seen to account well for the experimental points. The deviations at small  $t$  for 400 and particularly for 800 v are probably due to the inability of the carrier reservoir at the anode to continually supply the full SCLC values corresponding

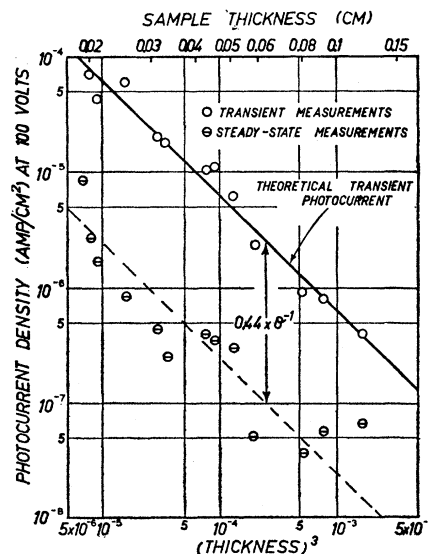


FIG. 7. Transient (circles) and steady-state (bisected circles) SCLC density for different samples plotted against the third power of their thickness. The solid line is computed from Eq. (1) ( $\mu=0.7$ ,  $\kappa=2$ ).

to these high voltages. According to the analysis of the case of slow trapping discussed in the preceding paper,<sup>2</sup> the decay characteristics of the SCLC should represent the carrier trapping kinetics. Apparently two types of trapping levels are present in this sample, with the slower decay component representing a redistribution of trapped carriers between shallow and deeper levels. Both types of levels are obviously characterized by very small capture cross sections.

Transient SCLC for a sample exhibiting much faster trapping is shown in Fig. 9. The points represent measurements at two applied voltages. The upper curve is again a theoretical plot for the case of no trapping ( $\tau = \infty$ ). It is immediately apparent that the experimental points fall well below this curve, indicating that some fast trapping processes, of time constant com-

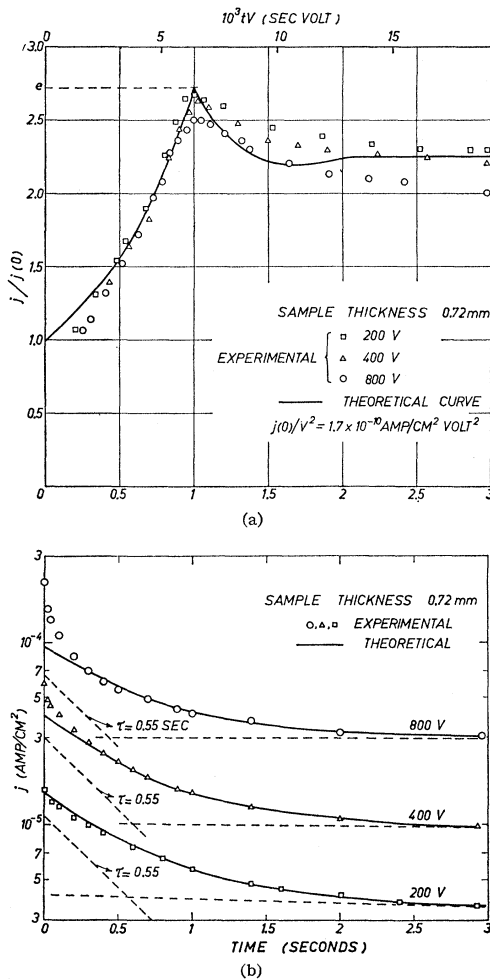


FIG. 8. (a) Transient SCLC arising from intense steady illumination, represented in dimensionless form, for three applied pulse-voltages;  $t_1$  is the transit time and  $j(0)$  the initial amplitude. The solid curve is a theoretical plot corresponding to no trapping ( $\tau = \infty$ ). (b) Transient SCLC density on the same sample but on a much larger time scale. The dashed curves represent the two decay components for each voltage; the solid curves represent the sums of corresponding components.

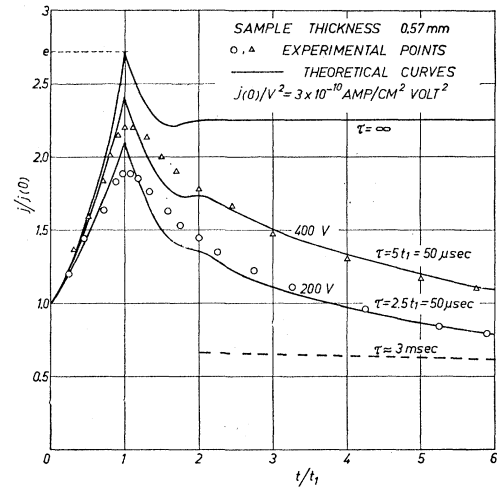


FIG. 9. Transient SCLC in a sample exhibiting pronounced trapping, represented in dimensionless form, for two applied pulse-voltages. The dashed curve represents the slow decay component. The two solid curves are computed theoretically<sup>2</sup>, with  $\tau/t_1$  equal to 2.5 and 5 for an applied voltage of 200 v and 400 v, respectively, and  $\theta_0 = 0.3$ . The calculated trapping time is 50  $\mu\text{sec}$ .

parable to the transit times  $t_1$ , play an important role in this case. A long component of the current decay is also present; its extrapolation to short times, for both voltages, is represented by the dashed line. On the time scale employed in the figure, this component is essentially a constant. For the analysis of the experimental data on this time scale we may therefore take an effective value of  $\theta_0$  as given by the ratio of the latter constant to the asymptotic value of  $j(t)$  in the absence of trapping ( $\tau = \infty$ ), i.e.,  $\theta_0 \approx 0.3$ . This effective  $\theta_0$  thus corresponds to the ratio of free to trapped charge attained after 10–20 transit times when quasi-stationary conditions have been established. Using this effective  $\theta_0$ , the two solid curves in Fig. 9, corresponding to 200 v ( $t_1 = 20 \mu\text{sec}$ ) and 400 v ( $t_1 = 10 \mu\text{sec}$ ) are computed from Eqs. (57) and (58) of the preceding paper,<sup>2</sup> with  $\tau/t_1 = 2.5$  and  $\tau/t_1 = 5$ , respectively. It is seen that the detailed SCLC characteristics for both voltages may be quite well accounted for by a single trapping time  $\tau = 50 \mu\text{sec}$ . The slower decay component corresponds again to some redistribution of charge between two types of levels.

### (b) Steady-State Measurements

We shall now discuss measurements of SCLC arising from an intense steady illumination of the anode under applied dc voltages. Compared to other materials iodine exhibits a unique behavior. Large sustained photocurrents are usually obtained even for samples over 1 mm thick. The holes thus have an exceedingly large range, indicating, once again, that trapping is very weak in this material. The steady-state SCLC is usually found to vary approximately as the square of the applied voltage. This behavior is characteristic to crystals

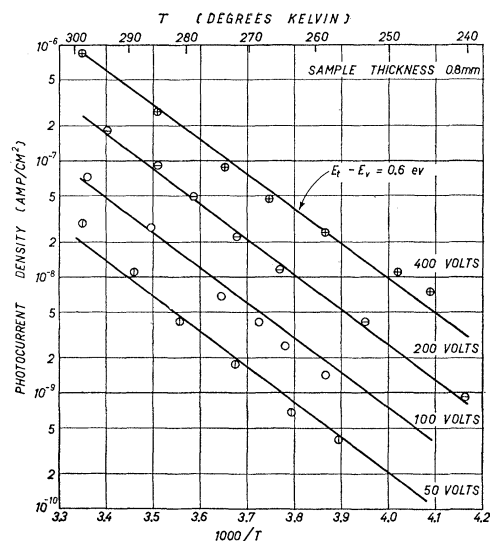


FIG. 10. The temperature dependence of the steady-state SCLC density for four applied dc voltages. The common slope yields the value of 0.6 ev for the position of the dominant trapping level above the valence-band edge.

having shallow traps.<sup>5,6</sup> The SCLC is then given by<sup>5,6</sup>

$$j(\infty) = 10^{-13} \theta \kappa \mu V^2 / L^3 \text{ amp/cm}^2, \quad (3)$$

where  $\theta = \theta_0 / (1 + \theta_0)$  is the fraction of the total space charge that is free. For the case of hole trapping at a single discrete set of levels,

$$\theta_0 = p/p_t = (N_v/N_t) \exp(-\Delta E/kT), \quad (4)$$

$N_v$  being the effective density of states in the valence band,  $N_t$  the concentration of traps, and  $\Delta E$  their energy position above the valence-band edge.

Figure 7, referred to previously, shows values of *transient* SCLC plotted against  $L^3$  for a number of different samples. Measurements of *steady-state* SCLC, also at 100-v applied voltage, were carried out on the *same* samples and are represented by the bisected circles. The large scatter of the points in this case is due to some variation in trap content from sample to sample (even though they were taken from the same batch). On the whole, however, the points are seen to conform well to the  $L^3$  dependence law (dashed curve). Inspection of Eqs. (1) and (3) shows that the distance between the solid and dashed curves should yield the value of  $0.44\theta^{-1}$  averaged over the samples studied. At room temperature, where these measurements were carried out, the average value of  $\theta$  is seen to be  $\sim 0.02$ .

The temperature dependence of the steady-state SCLC measured on one sample at four different applied voltages is shown in Fig. 10 on a semi-log scale. The points for the different applied voltages are equidistant, and exhibit the  $V^2$  dependence throughout the tempera-

ture range studied. Moreover, at any applied voltage the points lie approximately on a straight line, indicating that one discrete set of traps is dominant. As the temperature dependence of the hole mobility is relatively weak, the common slope yields essentially the energy position of the traps above the valence-band edge [Eqs. (3)–(4)]. For this particular sample  $\Delta E = 0.6$  ev (values obtained on a number of different samples range from 0.45 to 0.6 ev). Even if we take for the effective density of states in iodine  $N_v = 10^{22} \text{ cm}^{-3}$ , we obtain for the trap density for the case shown  $N_t = 5 \times 10^{13} \text{ cm}^{-3}$ . The actual density is probably lower by one or even two orders of magnitude. Using the results of transient measurements, one obtains for the order of magnitude of the capture cross section  $10^{-20} \text{ cm}^2$  or lower.

## V. DISCUSSION

A very good agreement has been shown to exist between the detailed characteristics of the observed transient SCLC in iodine and the theoretical predictions.<sup>2</sup> The theory accounts quantitatively for the initial amplitude of the transient SCLC and its dependence on applied voltage and sample thickness, as well as for the measured ratio of the transit times under space-charge and space-charge-free conditions. For weak trapping (Fig. 8) the observed shape of the SCLC follows closely the theoretical curve for  $\tau = \infty$ , with the ratio  $j(t_1)/j(0)$ , e.g., very nearly equal to  $e$ . The two basic assumptions of the mathematical analysis,<sup>1,2</sup> namely, that an ohmic contact is present (under intense illumination), and that the diffusive contribution to the total current may be neglected, are thus confirmed for the experimental conditions employed.

A similarly good agreement is obtained when trapping effects are prominent. This is demonstrated by the analysis of the results in Fig. 9 using the detailed theory presented in the preceding paper.<sup>2</sup> Here the same sample is studied at two different voltages (different  $t_1/\tau$ ). In both cases a good fit between theory and experiment is obtained by the use of the *same* value of the trapping time  $\tau$ . Such an analysis has been carried out on a large number of iodine samples and proved very useful in studying trapping kinetics.

The experimental evidence on iodine points to the following conclusions. The samples studied are all *p* type, with the Fermi level lying in an essentially trap-free void at about 1 ev above the valence-band edge. Upon illumination, the electrons are rapidly trapped, while the holes are distributed among the valence band and various trapping levels. For different samples the dominant hole traps are present with a density ranging from about  $10^{11}$  to  $10^{14} \text{ cm}^{-3}$  and situated between 0.45 and 0.6 ev. They are usually characterized by very low capture cross sections (of the order of  $10^{-20} \text{ cm}^2$ ). These traps are shallow in the sense that they lie below the steady-state Fermi level for all injection levels achieved in practice. The low trapping

<sup>5</sup> A. Rose, Phys. Rev. **97**, 1538 (1955).

<sup>6</sup> M. A. Lampert, Phys. Rev. **103**, 1648 (1956).

exhibited by most samples, in both transient and steady-state measurements, sets iodine apart from any known nonmolecular insulator. The large value of  $\theta$  ( $\sim 10^{-2}$  at room temperature) is to be contrasted, e.g., with the  $10^{-9}$  quoted<sup>7</sup> for CdS. Preliminary measurements on anthracene<sup>8</sup> suggest a similar behavior.<sup>9</sup> It is quite possi-

<sup>7</sup> R. W. Smith, RCA Rev. **20**, 69 (1959).

<sup>8</sup> M. Silver, M. Swicord, R. C. Jarnigan, A. Many, S. Z. Weisz, and M. Simhony, J. Phys. Chem. Solids **24** (1962).

<sup>9</sup> Note added in proof: Studies of SCLC in anthracene have also been reported by P. Mark and W. Helfrich [J. Appl. Phys. **33**, 205 (1962)].

ble that such a behavior is typical for molecular crystals.

In conclusion, it is believed that measurements of transient SCLC, especially when combined with steady-state measurements, constitute a powerful tool for the study of electronic processes in solids. This is particularly the case for materials characterized by low mobilities. At the same time, transient measurements under space-charge-free conditions seem promising in yielding information on such processes as surface recombination and carrier photogeneration in these materials.

## Theory of Exchange Relaxation of Hyperfine Structure in Electron Spin Resonance\*

JAMES D. CURRIN

*Institute of Theoretical Physics, Department of Physics, Stanford University, Stanford, California*

(Received January 29, 1962)

The electron spin exchange interaction between colliding molecules is examined as a possible relaxation mechanism for the hyperfine structure of free-radical molecules in solution. An expression is derived which, under suitable conditions, relates the frequency-dependent susceptibility to a single parameter  $q$ , which can be interpreted as the frequency of spin exchanges. For large values of  $q$  the absorption narrows to a single line of width  $\sigma^2/q$ , where  $\sigma$  is the mean square width of the unperturbed spectrum. For small values of  $q$  the widths of the individual hyperfine lines are found to depend upon their relative intensities. These results are compared with some recent experiments.

### I. INTRODUCTION

**E**LECTRON paramagnetic resonance spectra of many free radicals exhibit hyperfine splittings due to magnetic dipole coupling between the unpaired electron and magnetic nuclei within the molecule. This coupling consists of two contributions; the ordinary dipole-dipole interaction which is dependent upon the molecular orientation, and the "contact" interaction,  $a\mathbf{I}\cdot\mathbf{S}$ , between the nuclear spin  $\mathbf{I}$  and the electron spin  $\mathbf{S}$ , with the coupling constant  $a$  proportional to the electron charge density at the site of the magnetic nucleus. Typically, the hyperfine splittings are observed by dissolving the radical in a diamagnetic solvent, which reduces the intermolecular exchange and intermolecular dipole-dipole interactions to the point where the hyperfine structure is resolved. At sufficiently high temperatures, molecular tumbling averages the orientation-dependent part of the hyperfine coupling leaving only the contact interaction. If, in addition, the Larmor frequency due to the external magnetic field is much larger than the coupling constant  $a$ , then the electronic and nuclear spin can be separately space quantized and it is thus possible to treat the hyperfine coupling as a small increment to be added to the external magnetic field.

Our purpose in this paper is to examine in some detail a possibly important relaxation mechanism for these systems, namely, exchange interaction occurring during collisions between the free radical molecules. We will then attempt to apply our conclusions to some recent experimental results.

One method of attack on this problem would be to treat it as an application of a general theory of motional narrowing, as has been formulated, for example, by Kubo and Tomita.<sup>1</sup> One would then treat the hyperfine interaction as a perturbation which is modulated by the (time-dependent) exchange interaction. The "motional" Hamiltonian would then commute with the Zeeman Hamiltonian and also with the total electron magnetic moment and thus would obey the criteria for the applicability of motional narrowing theories. This approach would enable one to calculate the over-all second moment of the spectral intensity and in the case of strong motional narrowing ("fast motion") should represent the observed line shape quite well. It would not be of any use if one wished to study the various hyperfine lines individually. In this case the Zeeman and hyperfine interactions would have to be treated as a single unit which is perturbed by the exchange interaction. In the region intermediate between good hyperfine resolution and strong narrowing neither

\* Supported in part by the U. S. Air Force through the Air Force Office of Scientific Research.

<sup>1</sup> R. Kubo and K. Tomita, J. Phys. Soc. Japan **9**, 888 (1954).